Impact of Three Dimensional Atrial Fibrosis on Development and Stability of Rotational and Focal Sources in Atrial Fibrillation – A 3D Simulation and Clinical High-Density Mapping Study in Persistent Atrial Fibrillation

Markus Rottmann[1], Viktor Markstein[2], Ufuk Arslan[1], Heiko Lehrmann[2], Juergen Allgeier[2], Reinhold Weber[2], Wenzel Kaltenbacher[1], Olaf Dössel[1], Thomas Arentz[2], Amir S Jadidi[2]

[1]Institute of Biomedical Engineering, Karlsruhe Institute of Technology, Karlsruhe, Germany
[2]Arrhythmia Division, University Heartcenter Freiburg-Bad Krozingen, Germany

Abstract

The arrhythmogenic mechanisms of atrial fibrillation (AF) are still not well understood. Increased atrial fibrosis is a structural hallmark in patients with persistent AF. We assessed the electrogram signature rotational activity and their spatial relationship to low voltage areas in patients with persistent AF. Computer simulations implicating 3-dimensional atrial tissue with different amount of atrial fibrosis were used to assess development and stability of rotational activities during AF. Rotor anchoring occurred at the borderzone between fibrosis and healthy atrial tissue with 12 consecutive rotations prior to rotor extinction. Rotational activity in fibrotic tissue resulted in fractionated signals and were overlapped with large negative electrograms in unipolar recording mode from neighboring healthy tissue – impressing as a focal source. Necessary conditions for development and stability of rotational activities around fibrosis were on the one hand a minimum size of atrial fibrosis area equal or larger than 10mm x 10mm and on the other hand the degree of atrial fibrosis of 40%. Clinical data showed that AF termination sites were located within low voltage areas (displaying <0,5mV in AF on the multielectrode mapping catheter) in 80% and at their borderzones in 20% of cases.

1. Introduction

Today cardiovascular diseases are the number one cause of death. Atrial fibrillation (AF) is the most common human arrhythmia associated with increased risk for stroke, morbidity and mortality. Increased atrial fibrosis is a structural hallmark in patients with persistent AF. Recent clinical studies have revealed focal and rotational sources confined to pulmonary veins and specific areas of both atria in patients with persistent AF [1][3]. One hypothesis is that rotational sources or ectopic foci may drive AF and that arrhythmogenic sources may anchor at atrial region displaying low voltage and increased fibrosis [4]. The central question is what mechanisms are necessary for induction and maintenance of atrial fibrillation and what are the specific intracardiac signals that can be measured at those arrhythmia sources, in order to enable their identification via high-density mapping tools. Previously, a number of simulation studies have been performed on behaviour of rotational activities around obstacles or fibrotic tissue in 2D models of AF. We present data from the first simulation study of rotational activity during atrial fibrillation in a more realistic 3D atrial tissue model including 3-dimensional atrial fibrosis implemented at high resolution (0.1mm) with development of rotational activities at the 3D borderzone between fibrosis and healthy tissue. The rotated zig-zag excitation waves through the 3D fibrotic tissue and the focal source from fibrotic tissue to healthy tissue are in these simulation studies and offer new possibilities for understanding mechanisms and typical signal characteristics of AF drivers.

2. Methods

2.1. Simulation Setup

As cell model the Courtemanche Ramirez Nattel was used under AF conditions. Monodomain equations were solved with the parallel solver aCELLerate [6]. By forward calculation extracellular potentials were calculated with the sampling rate of 1000Hz.

Rotational Activity around a 3D Fibrosis Area

A stable rotational source around fibrosis was generated by a cross field protocol in an isotropic virtual 3D tissue patch with the dimensions of 30mm x 30mm x 2mm and spatial resolution of 0.1mm. Fibrosis was implemented in an area of 10mm x 10mm, compare figure 1. Locations and sizes of the passive fibrosis elements [7] were randomly distributed. Fibrosis elements measured 200µm in width

with variable lengths and heights described by Poisson distribution with λ=400µm [2].

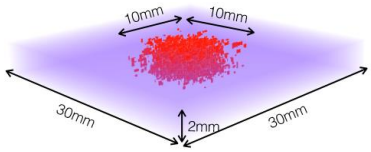

Figure 1. Fibrosis area (red) in tissue patch (purple).

Rotational Activity at the Borderzone between 3D Fibrosis and healthy Tissue

Rotational activity between fibrosis and healthy tissue was generated in the 3D patch (60mm x 60mm x 2mm) including a fibrotic area with increased fibrosis (45mm x 58mm x 2mm) of 40% [7], compare figure 6A. The stimulus protocol consisted on a plane wave from the left side and a second plane wave from the lower side 114.5ms later.

2.2. Cycle Length Coverage

Within one cycle length the parameter cycle length coverage (CLC) [5] was calculated with equation 1.

$$CLC = \frac{last\ LAT - first\ LAT}{cycle\ length}. \quad (5)$$

Equation 1

to the LAT obser

3. Results

3. Results

3.1. Rotational Activity was detected by CLC > 70% in clinical Mapping Data

Clinical mapping data included the analysis of termination sites in 45 persistent AF patients.

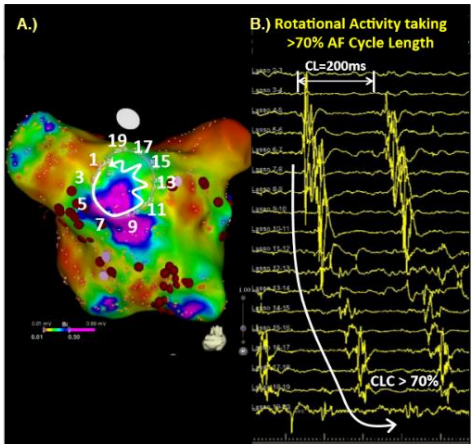

Figure 2. A. Peak to peak amplitude map of rotational activity measured with the Lasso catheter. B. Bipolar signals with the typical line pattern and repetitive CLC > 70%.

The majority (80%) of AF termination sites were located within low voltage areas <0,5mV in AF or at low voltage boderzones (20%). AF termination sites displayed repetitive CLC >70% on the Lasso or a 20-pole circular mapping catheter in 92% of cases and rapid focal activity in 8% of AF termination sites. Moreover, localized rotational activity was associated with the typical "line pattern" [5] on the circular mapping catheters, compare figure 2B.

3.2. Simulated rotational Activity around 3-dimensional atrial Fibrosis Area resulted in similar Signal Characteristics like in clinical Mapping Data

Rotational activity around 3D fibrosis was stable over time and resulted also within the fibrotic tissue in rotational zig zag movement. Inhomogeneous conduction within the region of increased fibrosis is revealed by "zig-zag" line pattern. Near the center of the fibrotic tissue there were over time continuous activated cells. This is the reason why electrodes at the fibrotic area center measured continuous fractionated signals. In simulation studies with less degree of fibrosis of 10% no anchoring of rotations was observed.

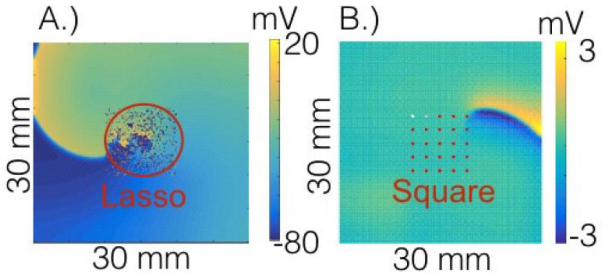

Figure 3. Rotational activity around 3D fibrosis area (dotted central area with 10mm x 10mm x 2mm dimension). The rotations were repetitive over time. Labyrinth like movement through fibrotic tissue resulted in continuous activated cells near the center of the fibrotic tissue.

Figure 4 shows the unipolar signals of the virtual Lasso catheter. The catheter center was in 4mm distance to the rotor tip. Fractionated signals were measured at the electrodes above the fibrotic tissue. Similar to the clinical case the typical line patterns of circular catheters were observed with repetitive CLC larger than 70% [4].
In the clinical peak to peak amplitude map, compare figure 2A, rotational activity occurred between atrial areas with higher fibrosis content (displaying bipolar peak-to-peak voltage <0,5mV) and the healthy atrial region at the posterior LA (>0,5mV in purple colour).

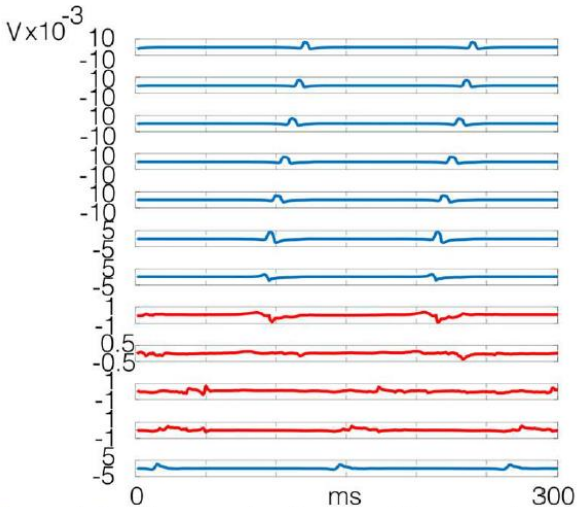

Figure 4: Bipolar signals of a virtual circular catheter in 4mm distance between catheter center and rotor tip position.

Both clinical and simulation data revealed repetitive AF cycle length coverage >70% within a 1cm radius around the core of rotational sources, typical line-like activation time pattern on multi-electrode catheter and partially continuous fractionated signals. A virtual square catheter, compare figure 3B, with 2mm electrode distance centered at the fibrotic tissue center measured the typical unipolar signal characteristics of rotational activity around fibrotic tissue, see figure 5. In the center electrode continuous fractionated signals with small amplitudes [5] of 0.1mV were measured.

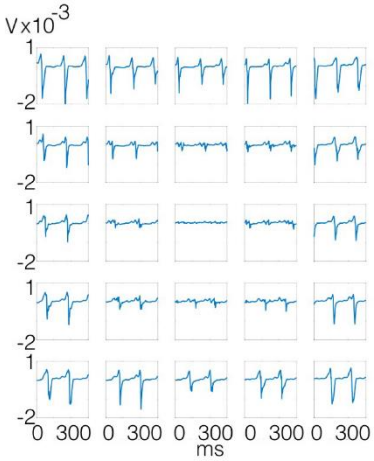

Figure 5. Unipolar signals of the square catheter with 2mm distance between 2 electrodes. Continuous fractionated signals with small amplitudes of 0.1mV were measured at the center of rotational activity.

3.3. Simulated rotational Activity at the Borderzone between 3-dimensional atrial Fibrosis Area and healthy Tissue

The rotational activity at the borderzone between healthy and fibrotic tissue was induced by two plane waves, from left and lower side, see figure 6A. In the first cycle the rotational activity moved into healthy tissue and anchored then over 12 cycles in the fibrotic tissue near the borderzone. A necessary condition for this anchoring was the degree of fibrosis of 40%. With smaller degree of fibrosis of 10% no anchoring resulted. In figure 6 it is particularly noteworthy that additional to the rotor tip position (marked in red), there were significant focal source points at exit points (marked in black) from fibrotic to healthy tissue.

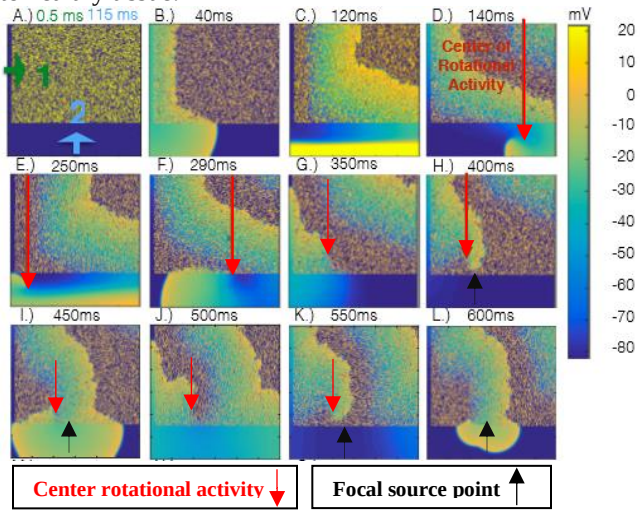

Figure 6. Rotational activity at the borderzone between fibrosis (yellow dots in upper layers) and healthy tissue (dark blue lower layers). The rotor tip (red) was stable over 12 cycles in fibrotic tissue near to the borderzone. Focal source point from fibrotic to healthy tissue (black).

Typical signal characteristics at the borderzone were measured with the square catheter, which was placed partially above fibrotic tissue (upper 3 columns) and partially above healthy tissue (lower 3 columns).

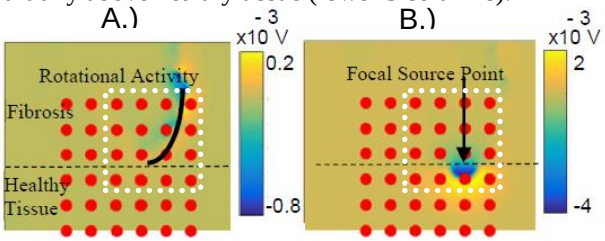

Figure 7. Square catheter with electrode distances of 2mm on A. partially circular excitation wave above fibrotic tissue. B. The focal source point from fibrotic to healthy tissue. The amplitudes at the focal sources in healthy tissue were nearly 10 times larger than measured signals above fibrotic tissue.

Figure 7A shows the rotational excitation wave front (black) in the low voltage area. There were focal sources at the border between fibrotic tissue and healthy tissue, compare figure 7B. Unipolar signals of the virtual square catheter, compare figure 7 (marked in white), are depicted in figure 8. Near to focal sources, i.e. at 780ms, strong negative amplitudes were measured. The large negative

amplitudes from the focal source overlapped the signals in fibrotic tissue (upper 3 columns), because of farfield effects at the same time points, compare exemplarily black dashed line and the rotor tip position in red, in figure 8.

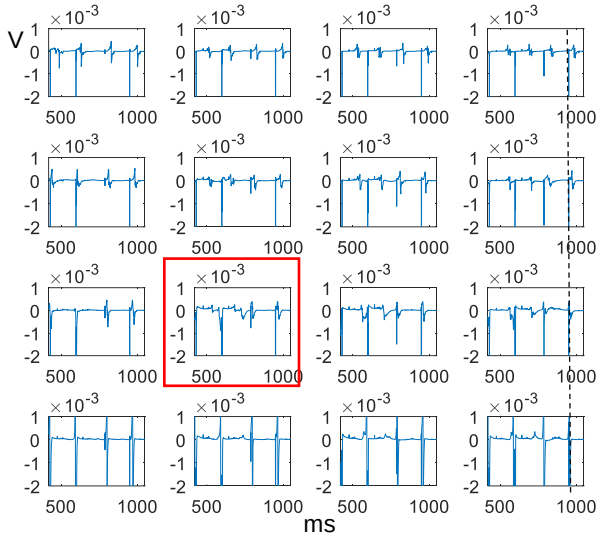

Figure 8. Unipolar signals of the placed square catheter. At the time points of the focal sources from fibrotic tissue to healthy tissue strong negative amplitudes were measured (marked in black). The rotor tip position is marked in red.

In the upper 3 columns of the virtual square catheter the signal potentials of the zig zag rotational excitation through the 3D fibrotic tissue resulted in fractionated signals, compare figure 8, with overlapping strong negative amplitude caused by the focal source between fibrotic and healthy tissue.

4. Discussion and Summary

This work presents a simulation study of extracellular potentials of rotational activity during AF within potentials of rotational activity within an atrial model including regional 3D fibrosis. Using the 3D atrial model with regional fibrosis, we could observe anchoring and stabilization of rotational activity during fibrillatory activity at the borderzone between 3D fibrosis and healthy tissue. Furthermore this simulation study shows that continuous fractionated signals were measured at the tip of rotational activity occurring within borderzones of 3D atrial fibrosis areas. Necessary conditions for development and stability of rotational activities around fibrosis were on the one hand a minimum size of atrial fibrosis area equal or larger than 10mm x 10mm and on the other hand a degree of atrial fibrosis of 40%. Rotational activity occurred between fibrosis and healthy tissue and was stable over 12 AF cycles. This study shows that atrial areas with increased fibrosis and their border zones could induce and maintain AF. Clinical data showed that AF termination sites were located within low voltage areas (displaying <0,5mV in AF on the multi-electrode mapping catheter) in 80% and at their borderzones in 20% of cases. The different hypotheses that AF is driven by re-entries, rotors or focal sources might be explained by the presented 3D simulation study and support clinical data with AF termination at low voltage sites. On the one hand rotational activity can be measured in fibrotic tissue, but the signals are fractionated and may overlap with large negative signals from neighbouring healthy tissue – impressing as a focal source with large negative electrograms in unipolar recording mode. In future, identification of pro-arrhythmogenic atrial regions with increased fibrosis and decreased voltage harbouring rotational and focal sources should be improved, in order to further advance diagnosis and therapeutic options for patients with AF.

References

[1] Natale A, Jalife R. Atrial Fibrillation. From Bench to Bedside. Totowa: Humana Press, 2008.

[2] Spach MS, Heidlage JF, Dolber PC, et al. Mechanism of origin of conduction disturbances in aging human atrial bundles: experimental and model study. Heart Rhythm 2007;4:175–185.

[3] Haissaguerre M, Hocini M, Sanders P, Takahashi Y, Rotter M, Sacher F, Rostock T, Hsu LF, Jonsson A, O'Neill MD, Bordachar P, Reuter S, Roudaut R, Clementy J, Jais P. Localized sources maintaining atrial fibrillation organized by priorablation. Circulation 2006;113:616–625.

[4] Jadidi A, Lehrmann H, Sorrel J, Minners C, Park C, Keyl C, Denis A, Jais P, Hocini M, Markstein V, Potocnik C, Allgeier J, Hochholzer W, Herrera-Sidloky C, El Omri Y, Neumann F, Weber R, Haissaguerre M, Arentz T. Ablation of persistent atrial fibrillation targeting low voltage areas with selective electrogram characteristics. Circulation Arrhythmia and Electrophysiology, 2016.

[5] Rottmann M, Unger L, Kaltenbacher W, Seemann G, Loewe A, Krueger MW, Jadidi A, Arentz T, Dössel O. Methods for analyzing signal characteristics of stable and unstable rotors in a realistic heart model. Computing in Cardiology 2015;43:485–488.

[6] Seemann G, Sachse FB, Karl M, Weiss DL, Heuveline V, Doessel O. Framework for modular, flexible and efficient solving the cardiac bidomain equation using petsc. Mathematics in Industry 2010;15:363–369.

[7] Keller M. W, Luik A, Soltan Abady M, Seemann G, Schmitt C, Dössel. Influence of three-dimensional fibrotic patterns on simulated intracardiac electrogram morphology. Computing in Cardiology 2013;40: 923-926.

[8] Rottmann M, Keller MW, Oesterlein T, Seemann G, Dössel O. Comparison of different methods and catheter designs to estimate the rotor tip position - a simulation study. Computing in Cardiology 2014:41:133–136.

Address for correspondence:
Markus Rottmann,
Kaiserstr. 12,
76128 Karlsruhe,
publications@ibt.kit.edu